



EVALUATION OF THE USE OF OPTICAL FIBER THERMOMETERS FOR THERMAL CONTROL OF THE QUENCH MODULE INSERT

Matthew R. Jones

Department of Aerospace and Mechanical Engineering
The University of Arizona

Jeffrey T. Farmer

Marshall Space Flight Center
NASA

Shawn P. Breeding

Tec-Masters, Inc.

ABSTRACT

Issues regarding the use of optical fiber thermometers to control heater settings in a microgravity vacuum furnace are addressed. It is desirable to use these probes in environments such as the International Space Station, because they can be operated without re-calibration for extended periods. However, the analysis presented in this paper shows that temperature readings obtained using optical fiber thermometers can be corrupted by emissions from the fiber when extended portions of the probe are exposed to elevated temperatures.

INTRODUCTION

The Quench Module Insert (QMI) is a platform for conducting solidification experiments in a microgravity environment. Current plans call for the installation of the QMI in the Microgravity Science Research Rack #1 on the International Space Station. The design of the QMI is similar to that of a Bridgman furnace and consists of a heater core, insulation jacket, instrumentation, coolant loop components, and a quench system. The QMI hot zone assembly is shown in Figure 1. The heater core contains four heated zones: Booster 1, Booster 2, Main and Guard. The sensor plate is cooled in order to maintain the optical fiber thermometers (OFT) and other instrumentation at acceptable operating temperatures. The quenching occurs in a water-cooled chill block (not shown) which is located adjacent to Booster 1. This design produces the high thermal gradients required for directional solidification processing experiments.

Precise thermal control is necessary to perform the candidate experiments for the QMI, and there is concern that thermocouples will drift due to exposure to cyclical thermal environments during the extended period of time it is planned to have the QMI in orbit. This concern led to the inclusion of OFT in the design of the QMI. Preliminary designs call for the installation of Accufibers with sapphire blackbody sensors. Accufibers are a brand of OFT manufactured by LUXTRON Corporation. Product literature available from LUXTRON indicates that Accufibers have an accuracy of 0.2% at 1000 C and a resolution of 0.01 C. In

addition, Accufibers demonstrate excellent long-term stability and are immune to electromagnetic interference. In the proposed QMI design, the sapphire fiber is aligned with the axis of the QMI and an extended portion of the fiber is exposed to elevated temperatures. The analysis presented in this paper indicates that OFT readings will be corrupted under these conditions. Results obtained from a thermal model of the QMI are used to predict the temperature readings of an OFT probe. These predictions are consistent with readings obtained during the testing of a QMI prototype.

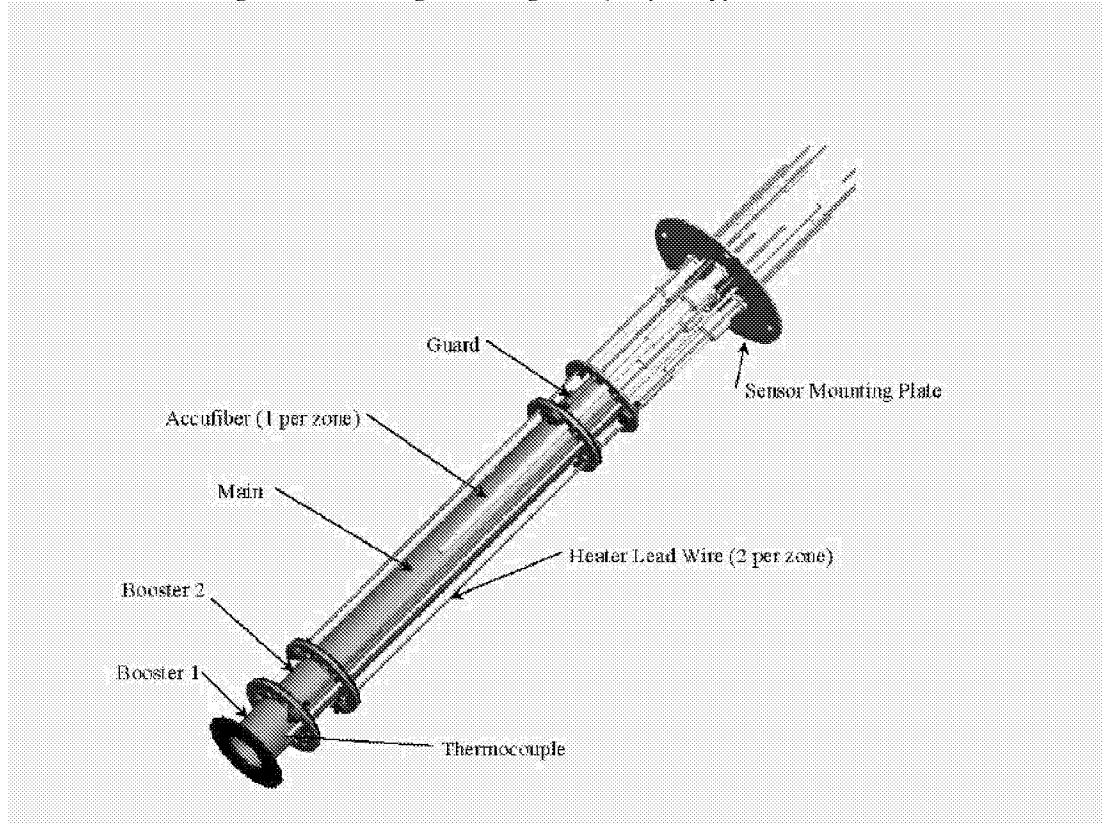


Figure 1: QMI Hot Zone (Heater Elements) Assembly¹.

OVERVIEW OF OPTICAL FIBER THERMOMETRY

This section summarizes the basic principles of OFT². An Accufiber sapphire blackbody sensor is illustrated in Figure 2. The probe consists of a sapphire (Al_2O_3) fiber whose sensing tip is given a metallic coating. The sensing tip of the fiber is essentially an isothermal cavity, so the emission from this cavity will be approximately equal to the emission from a blackbody. The other end of the fiber is attached to the OFT detection system.

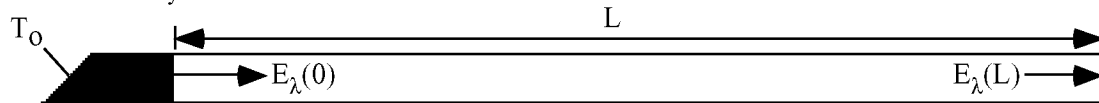


Figure 2: Schematic diagram for an Accufiber sapphire blackbody sensor. The sensing tip ($z=0$) is coated with a thin metallic film to create a small isothermal cavity at a temperature of T_0 . The radiative flux emitted by the cavity, $E_\lambda(0)$, is approximately equal to the spectral emissive power of a blackbody, $E_{b\lambda}(T_0)$.

Modeling the sapphire fiber as a non-scattering medium, the radiative flux propagating along the fiber is governed by³

$$\frac{dE_\lambda}{dz} = -K_{a\lambda}E_\lambda + K_{a\lambda}E_{b\lambda}(T(z)) \quad (1)$$

where E_λ is the spectral radiative flux ($\text{W}/\text{m}^2 \mu\text{m}$), $K_{a\lambda}$ is the spectral absorption coefficient (mm^{-1}) and $E_{b\lambda}(T(z))$ is the spectral emissive power of a blackbody at a temperature of $T(z)$. If the spectral absorption coefficient is independent of temperature, it is convenient to use the optical depth as the independent variable

$$t_\lambda = K_{a\lambda}z \quad (2)$$

Eq. (1) then becomes

$$\frac{dE_\lambda}{dt_\lambda} + E_\lambda = E_{b\lambda}(T(t_\lambda)) \quad (3)$$

Assuming that the sensing tip of the probe emits like a blackbody, the appropriate boundary condition for Eq. 3 is

$$E_\lambda(0) = E_{b\lambda}(T_0) \quad (4)$$

The solution to Eq. 3, subject to the boundary condition given by Eq. 4 is

$$E_{b\lambda}(T_0) = E_\lambda(t_{\lambda L}) \exp\{t_{\lambda L}\} - \int_0^{t_{\lambda L}} E_{b\lambda}(T(t_\lambda)) \exp\{t_\lambda\} dt_\lambda \quad (5)$$

where $t_{\lambda L} = K_{a\lambda}L$. The spectral radiative flux measured by the Accufiber detection system, M_λ , is related to the spectral radiative flux at the end of the sapphire fiber.

$$M_\lambda = E_\lambda(t_{\lambda L}) \Delta\lambda C \quad (6)$$

where $\Delta\lambda$ is the width of the band pass filter used by the Accufiber probe and C is a correction factor to account for various losses in the detection system. Substitution of Eq. 6 into Eq. 5 gives

$$E_{b\lambda}(T_0) = \frac{M_\lambda e^{t_{\lambda L}}}{\Delta\lambda C} - \int_0^{t_{\lambda L}} E_{b\lambda}(T(t_\lambda)) \exp\{t_\lambda\} dt_\lambda \quad (7)$$

The integral on the right hand side of Eq. 7 represents the portion of the measured spectral radiative flux that is due to emission by the fiber. This integral can be neglected if sapphire is a poor emitter at the wavelengths of interest ($K_{a\lambda} \ll 1$) or if the fiber is at a low enough temperature to ensure that the emission by the fiber is negligible at the wavelengths of interest ($T(t_\lambda) \ll T_0$).

The spectral emissive power of a blackbody at a temperature of T is given by Planck's equation.

$$E_{b\lambda}(T) = \frac{c_1}{\lambda^5 \left[\exp\left\{\frac{c_2}{\lambda T}\right\} - 1 \right]} \quad (8)$$

where the radiation constants are $c_1 = 3.7413 \times 10^8 \text{ W}\mu\text{m}^4/\text{m}^2$ and $c_2 = 14388 \mu\text{mK}^3$. For the wavelengths used by the Accufiber probe ($\lambda_1 = 0.80 \mu\text{m}$, $\lambda_2 = 0.95 \mu\text{m}$) and the temperature range of interest (400 - 1700 K), the exponential term is much larger than one. Therefore, Eq. 8 is well approximated using Wein's limit.

$$E_{b\lambda}(T) \approx \frac{c_1}{\lambda^5 \exp\left\{\frac{c_2}{\lambda T}\right\}} \quad (9)$$

The temperature reading obtained by the Accufiber probe, T_m , is calculated by neglecting the integral in Eq. 7. Substitution of Eq. 9 into Eq. 7 then gives

$$\exp\left\{-\frac{c_2}{\lambda T_m}\right\} = \frac{\lambda^5 M_\lambda e^{t_{\lambda L}}}{c_1 \Delta \lambda C} \quad (10)$$

Using the measurements at two wavelengths and Eq. 10, the following ratio can be formed.

$$\frac{\exp\left\{-\frac{c_2}{\lambda_1 T_m}\right\}}{\exp\left\{-\frac{c_2}{\lambda_2 T_m}\right\}} = \left(\frac{\lambda_1}{\lambda_2}\right)^5 \left(\frac{C \Delta \lambda_2}{C \Delta \lambda_1}\right) \left(\frac{M_{\lambda_1} e^{t_{\lambda_1 L}}}{M_{\lambda_2} e^{t_{\lambda_2 L}}}\right) \quad (11)$$

Assuming that $\Delta \lambda_1 \approx \Delta \lambda_2$ and that the losses in the Accufiber detection system do not depend on wavelength, T_m is given by

$$T_m = \frac{c_2}{(\lambda_2 - \lambda_1) \ln \left[\left(\frac{\lambda_1}{\lambda_2}\right)^5 \left(\frac{M_{\lambda_1} e^{t_{\lambda_1 L}}}{M_{\lambda_2} e^{t_{\lambda_2 L}}}\right) \right]} \quad (12)$$

ANALYSIS OF ERRORS DUE TO EMISSION BY THE FIBER

Clearly, temperatures obtained using Eq. 12 will only be accurate when the approximations employed in the derivation are satisfied. In particular, emission by the fiber will change the value of the radiative flux measured by the OFT detection system and result in inaccurate measurements when large portions of the sapphire fiber are at elevated temperatures.

RELATIONSHIP BETWEEN T_o AND T_m

Recall that the measured temperature is the temperature obtained when the integral in Eq. 7 is neglected. The relationship between the measured spectral radiative flux and the measured temperature is

$$\frac{M_\lambda e^{t_{\lambda L}}}{\Delta \lambda C} = \frac{c_1}{\lambda^5} \exp\left\{-\frac{c_2}{\lambda T_m}\right\} \quad (13)$$

Substituting Eq. 13 into Eq. 7 and solving for T_m gives

$$T_m = \frac{c_2 \left(\frac{1}{\lambda_2} - \frac{1}{\lambda_1}\right)}{\ln \left[\exp\left\{-\frac{c_2}{\lambda_1 T_o}\right\} + f(\lambda_1, T(t_{\lambda_1})) \right] - \ln \left[\exp\left\{-\frac{c_2}{\lambda_2 T_o}\right\} + f(\lambda_2, T(t_{\lambda_2})) \right]} \quad (14)$$

where

$$f(\lambda, T(t_\lambda)) = \frac{\lambda^5}{c_1} \int_0^{t_{\lambda L}} E_{b\lambda}(T(t_\lambda)) \exp\{t_\lambda\} dt_\lambda \quad (15)$$

and $T(t_\lambda)$ is the temperature profile along the sapphire fiber.

In order to evaluate Eq. 14 and assess the errors due to emission by the fiber, it is necessary to know the temperature profile along the fiber and the absorption coefficient of Al_2O_3 at the wavelengths of interest. The following sections address these matters.

TEMPERATURE PROFILE ALONG THE OPTICAL FIBER THERMOMETER

The OFT probes are inserted in a boron nitride sleeve that surrounds the heated core of the QMI. The probes are coupled radiatively to the sleeve in which they are housed. There is also a conduction path along the fibers to the sensor mounting plate. A SINDA model of the thermal environment of each fiber was developed to estimate the temperature profile along the fiber. A description of the geometry of the QMI and the SINDA thermal model is given elsewhere¹.

The SINDA model was used to calculate simulated OFT readings for the probes that are aligned with the Booster 1, Booster 2 and Main heating elements for the six cases listed in Table 1. The set points refer to the temperatures settings of the heating elements. Since the sensing tips of the OFT are positioned in the boron nitride sleeve and away from the heating elements, the set points are 10 to 40 C higher than the temperatures of the sensing tips. Figures 3 - 5 show the estimated temperature profiles for each of the three OFT probes.

Table 1. QMI Heater Set Points

Case	Booster 1 Set Point (C)	Booster 2 Set Point (C)	Main Set Point (C)	Guard Set Point (C)
1	600	600	600	600
2	600	600	650	650
3	900	900	900	900
4	900	900	950	950
5	1100	1100	1100	1100
6	1200	1150	1100	1100

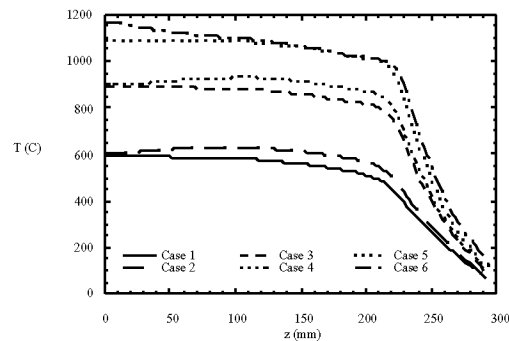


Figure 3: Estimated temperature profiles for Probe 1.

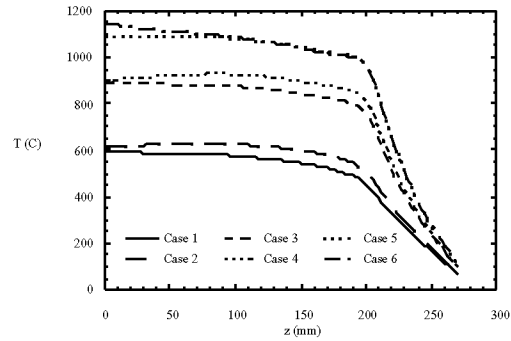


Figure 4: Estimated temperature profiles for Probe 2.

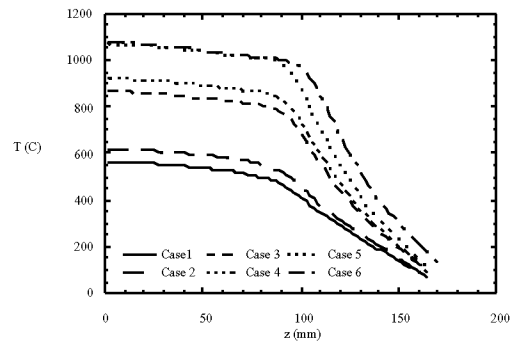


Figure 5: Estimated temperature profiles for Probe 3.

OPTICAL PROPERTIES OF SAPPHIRE

Brewster³ lists values for the real and imaginary parts of the refractive index a function of wavelength. At 1 μm , the imaginary part of the refractive index is $k = 6 \times 10^{-8}$. Assuming that the refractive index does not vary significantly with wavelength, the absorption coefficients at 0.80 and 0.95 μm can be calculated.

$$K_{a\lambda_1} = \frac{4\pi k}{\lambda_1} = 9.42 \times 10^{-4} \text{ mm}^{-1} \quad (16)$$

$$K_{a\lambda_2} = \frac{4\pi k}{\lambda_2} = 7.94 \times 10^{-4} \text{ mm}^{-1} \quad (17)$$

These values are consistent with the data published by Gryvnak and Burch⁴ as shown in Figure 6.

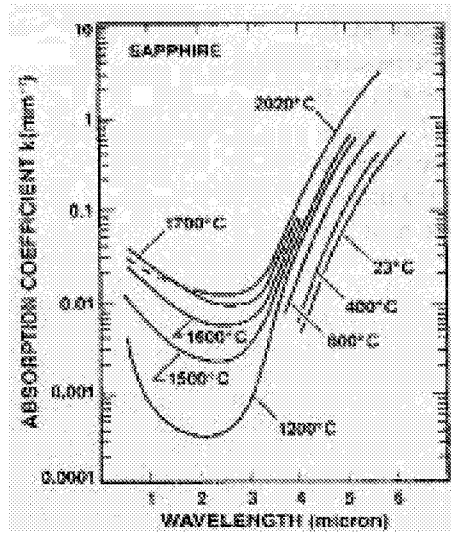


Figure 6: Spectral absorption coefficient of single crystal sapphire (Al_2O_3) at elevated temperatures⁴.

COMPARISON OF T_o AND T_m

Using the estimated temperature profiles shown in Figures 3 - 5 and the spectral absorption coefficients given by Eq. 16 and Eq. 17, the integral in Eq. 15 was evaluated numerically. Estimates for T_m were then calculated for each of the OFT temperature profiles. These values are compared with the temperature at the sensing tip of the OFT in Table 2.

Table 2. Comparison of OFT Readings and Sensing Tip Temperatures

Probe	Case	OFT Readings (C)	OFT Sensing Tip Temperature (C)
1	1	598	594
1	2	616	604
1	3	900	890
1	4	916	896
1	5	1102	1087
1	6	1171	1167
2	1	595	592
2	2	621	612
2	3	898	891
2	4	920	903
2	5	1100	1087
2	6	1145	1142
3	1	563	561
3	2	618	616
3	3	869	866
3	4	924	920
3	5	1075	1071
3	6	1085	1080

Comparison of the predicted OFT readings with the estimated sensing tip temperatures indicates that errors due to fiber emission increase as the length of fiber exposed to elevated temperatures increases. These results also show that the errors increase as temperatures increase.

COMPARISON OF PREDICTED AND MEASURED OFT TEMPERATURES

A prototype version of the QMI was tested at various heater settings, and the OFT readings were obtained for the six cases listed in Table 1. These measured values are compared with the predicted values in Table 3.

Table 3. Predicted and Measured OFT Temperature Readings

Probe	Case	Predicted OFT Temperature Reading (C)	Measured OFT Temperature Reading (C)
1	1	598	586
1	2	616	591
1	3	900	873
1	4	916	879
1	5	1102	1064
1	6	1171	1132
2	1	595	612
2	2	621	639
2	3	898	910
2	4	920	938
2	5	1100	1115
2	6	1145	1146
3	1	563	576
3	2	618	620
3	3	869	857
3	4	924	904
3	5	1075	1052
3	6	1085	1059

The agreement between the measured and predicted OFT readings is somewhat imprecise. The measurements obtained from probe 1 are consistently lower than the predicted values. Measurements obtained using probe 2 are consistently higher than the predicted values. Since the temperatures in the boron nitride sleeve vary considerably, these results indicate that the location of the probe's sensing tips in the QMI prototype may differ from their location in the SINDA model. In addition, uncertainties regarding the thermal coupling between the OFT probes and their environment in the SINDA model make a precise interpretation of these results difficult.

SUMMARY AND CONCLUSIONS

The analysis presented in this paper demonstrates that an elevated temperature profile along the fiber will increase the temperature read by an OFT system due to radiative emission by the fiber. An expression that quantifies the errors due to fiber emission has been derived. The results presented in this paper show that the difference between the measured and tip temperatures decreases as the length of fiber exposed to elevated temperatures decreases. Also, the errors generally increase as temperatures increase.

Predictions of the OFT readings based on a SINDA model of the probes thermal environment were compared with OFT readings obtained during the testing of a prototype of the QMI. The agreement between the predicted and measured values is not exact, but is consistent with uncertainties regarding the exact position of the sensing tips of the probes and the thermal coupling between the probes and their surroundings. Efforts to more accurately characterize the thermal environment of the OFT are currently being made.

ACKNOWLEDGMENTS

MRJ wishes to acknowledge the support of NASA - Marshall Space Flight Center through an Intergovernmental Personnel Act Assignment Agreement.

REFERENCES

1. NASA-MSFC, Tec-Masters, Inc., Sverdrup Technologies 1999 *Thermal Design Data Book*, Quench Module Insert, Preliminary Design Review.
2. Dils, R. R. 1983 "High-temperature optical fiber thermometry," *Journal of Applied Physics*, Vol. 54 (3), pp. 1198-1201.
3. Brewster, M. Q. 1992 *Thermal Radiative Transfer & Properties*, John Wiley & Sons, New York.
4. Gryvnak, D. A. and Burch, D. E. 1965 "Optical and Infrared Properties of Al₂O₃ at Elevated Temperatures," *Journal of the Optical Society of America*, Vol. 55 (6) pp. 625-629.